Comparison of Precipitation Projections of CMIP5 and CMIP6 Global Climate Models over Yulin, China

Mohammed Sanusi Shiru
Federal University Dutse
Eun-Sung Chung (eschung@seoultech.ac.kr)
Seoul National University of Science and Technology https://orcid.org/0000-0002-4329-1800
Shamsuddin Shahid
Universiti Teknologi Malaysia
Xiao-Jun Wang
Nanjing Hydraulic Research Institute

Research Article

Keywords: CMIP6, climate change, global circulation model, statistical indices, Yulin

Posted Date: June 17th, 2021

DOI: https://doi.org/10.21203/rs.3.rs-628014/v1

Corresponding Author

Eun-Sung Chung

Professor, Seoul National University of Science and Technology

Email: eschung@seoultech.ac.kr

Comparison of Precipitation Projections of CMIP5 and CMIP6 Global Climate Models over Yulin, China

Mohammed Sanusi Shiru[1,2], Eun-Sung Chung[1*], Shamsuddin Shahid[3], Xiao-Jun Wang[4]

[1] Department of Civil Engineering, Seoul National University of Science and Technology, Seoul 01811, South Korea.

[2]Department of Environmental Sciences, Faculty of Science, Federal University Dutse, P.M.B 7156, Dutse, Nigeria.

[3]Department of Water and Environmental Engineering, School of Civil Engineering, Faculty of Engineering, Universiti Teknologi Malaysia (UTM), 81310 Johor Bahru, Malaysia

[4] State Key Laboratory of Hydrology-Water Resources and Hydraulic Engineering, Nanjing Hydraulic Research Institute, Nanjing 210029

*Correspondence: eschung@seoultech.ac.kr

Comparison of Precipitation Projections of CMIP5 and CMIP6 Global Climate Models over Yulin, China

Abstract

This study compared precipitation projections of Coupled Model Intercomparison Project 5 (CMIP5) and 6 (CMIP6) GCMs over Yulin City, China. The performance of CMIP5 and CMIP6 GCMs in replicating Global Precipitation Climatology Centre (GPCC) precipitation climatology of the city was evaluated using different statistical metrics. The best performing GCMs common to both CMIP5 and CMIP6 were selected and subsequently downscaled to GPCC resolution using linear scaling method to spatiotemporal changes in precipitation. The study revealed BCC.CSM1.1(m), IPSL.CM5A.LR, MRI.CGCM3 and MIROC5 of CMIP5 and their equivalents BCC-CSM2-MR, IPSL-CM6A-LR, MRI.ESM2.0 and MIRCO6 of CMIP6 as the most suitable GCMs for the projection of rainfall in Yulin. Changes in precipitation were in the range of -14.0 – 0.0% and -22.0 – 0.2% during 2021–2060 for RCP4.5 and SSP2-4.5 respectively. The highest decrease of -29.7 − -22.0% was projected by MRI-ESM-2-0 for SSP2-4.5, while -28.0 – -20.0% by MIROC5 for RCP4.5. For RCP8.5 and SSP5-8.5, precipitation was projected to decrease in the range of -17.0 − -2.0% and -32.0 − 0.0%, respectively during 2021 − 2060 by most of the GCMs. An increase in precipitation up to 12.3% was projected only by IPSL-CM5A-LR for RCP8.5 for this period. The highest decrease was projected by MIROC5 (-40.2 – -29.0%) for RCP8.5 and IPSL-CM6A-LR (-40.2 – -26.0%) for SSP5-8.5. Overall, the results revealed a higher decrease in precipitation in Yulin city by CMIP6 GCMs compared to those projected by their corresponding GCMs of CMIP5 for both scenarios.

Keywords: CMIP6, climate change, global circulation model, statistical indices, Yulin

1. Introduction

Climate change has been an issue of concern over several decades due to its devastating impacts. It has increased the risks of flooding (Manawi et al., 2020; Rahman et al., 2019), occurrences of droughts (Alamgir et al., 2019; Ayugi et al., 2020; Shiru et al., 2019a), heatwaves (Kang and Eltahir, 2018; Khan et al., 2019; Satyanarayana and Rao, 2020) and ecosystem damages (Kim et al., 2019; Pérez-Ruiz et al., 2018). Many sectors including water resources, agriculture, energy and health among others have also been affected by the changing climate.

Like many other parts of the globe, China is also experiencing the impacts of climate change. Flooding is a common occurrence in different parts of China including cities like Yulin (Huang et al., 2015; Yang et al., 2017) and it often causes damages to sectors such as power, agriculture, health and sometimes leads to loss of lives (He et al., 2018). In 2003, heavy precipitation caused river flooding leading to the destruction of 17,438 acres of farmlands, destruction of roads, and damages to about 1,458 houses (He et al., 2018). Heavy precipitation affected more than 150,000 people in 2012 with 15 people missing and11 deaths, destruction of roads and disruption of aviation due to the heavy rain (China-Daily 2012). The disaster caused a direct economic loss in the Yulin and Yan'an region up to 134 million yuan ($21 million). Similarly, the flood in 2016 affected more than 21,000 people and evacuation of about 1200 persons (He et al., 2018). The flood led to the damage of more than 850 houses, destruction of more than 1100 kilometers of roads, damages to 30 bridges and culverts, and caused 11 landslides and other related geological disasters. The economic implication of the disaster was about 150 million yuan. The region is also known to be affected by droughts (Wang et al., 2020; Yin et al., 2020).

Understanding the expected changes in climate is crucial for the areas susceptible to disasters in order to develop adaptation and mitigation plans against climate change. This is particularly important using the recently released global climate models (GCM) of the Coupled Model Inter-comparison Phase 6 (CMIP6). It is also crucial to assess how the CMIP6 differ in projection from the previous Coupled Model Inter-comparison Phase 5 (CMIP5) in order to streamline the existing adaptation measures based on CMIP5 projections (Jiang et al., 2020; Song et al., 2021).

GCMs are developed by different institutions and have different performances in different parts of the globe (Chen et al., 2017). Hence, the selection of the most realistic ones for a reliable projection of climate for a region is crucial. The assessment of the performances of GCMs has

been conducted using different statistical indices (Rivera and Arnould, 2020; Sreelatha and Anand Raj, 2019). However, due to contradictory outputs from different statistical measures, supporting such outputs with other measures can be beneficial in reaching a compromise.

As GCMs are characterized by coarser spatial resolutions, their applications in climate projections and climate change impact studies at local and regional scales can be unreliable (Onyutha et al., 2016; Pour et al., 2018; Salman et al., 2018). Therefore, they are required to be downscaled (Almazroui et al., 2020a; Sa'adi et al., 2019; Shiru et al., 2020) using either the dynamical downscaling or the statistical downscaling (SD) methods. The SD method is known to have the advantages of computational efficiency and cost-effectiveness, the possibility of incorporation of observations directly into methods, and provision of point-scale climatic projections from GCM-scale (Fowler et al., 2007).

An array of statistical metrics was used to select the best performing GCMs for the projection of precipitation in the study area. Equivalent GCMs of the CMIP5 and CMIP6 for selected for the comparison of projections. The selected GCMs were downscaled using linear scaling method. This study employs only the GCMs which can reliably simulate the exiting climate of the study area and thus, capable to provide a trustworthy comparison of CMIP5 and CMIP6 projects. It is expected that the comparison of precipitation projections of CMIP5 and CMIP6 would help in streamlining the existing adaptation measures formulated based on CMIP5 projections or deriving new measures based on new scenarios of CMIP6.

2. Study Area and Datasets

2.1. Study Area

The study area, Yulin (Figure 1) is located in the northern Shaanxi province of China (Longitude: 107°15′47″–111°14′44″E; Lattitude: 36°49′07″–39°34′47″N). Yulin covers a total area of 385 km by 263 km (Zha, et al. 2008). The terrain of the area descends from 1,907 m in the east to 585 m in the west above the mean sea level. Yulin has a semi-arid temperate continental monsoon type climate which is characterized by dry and little precipitation in spring and winter and high precipitation during summer and autumn. The annual average precipitation in Yulin is around 450 mm. The annual average temperature in the area is 9.6°C (Wang, 2016).

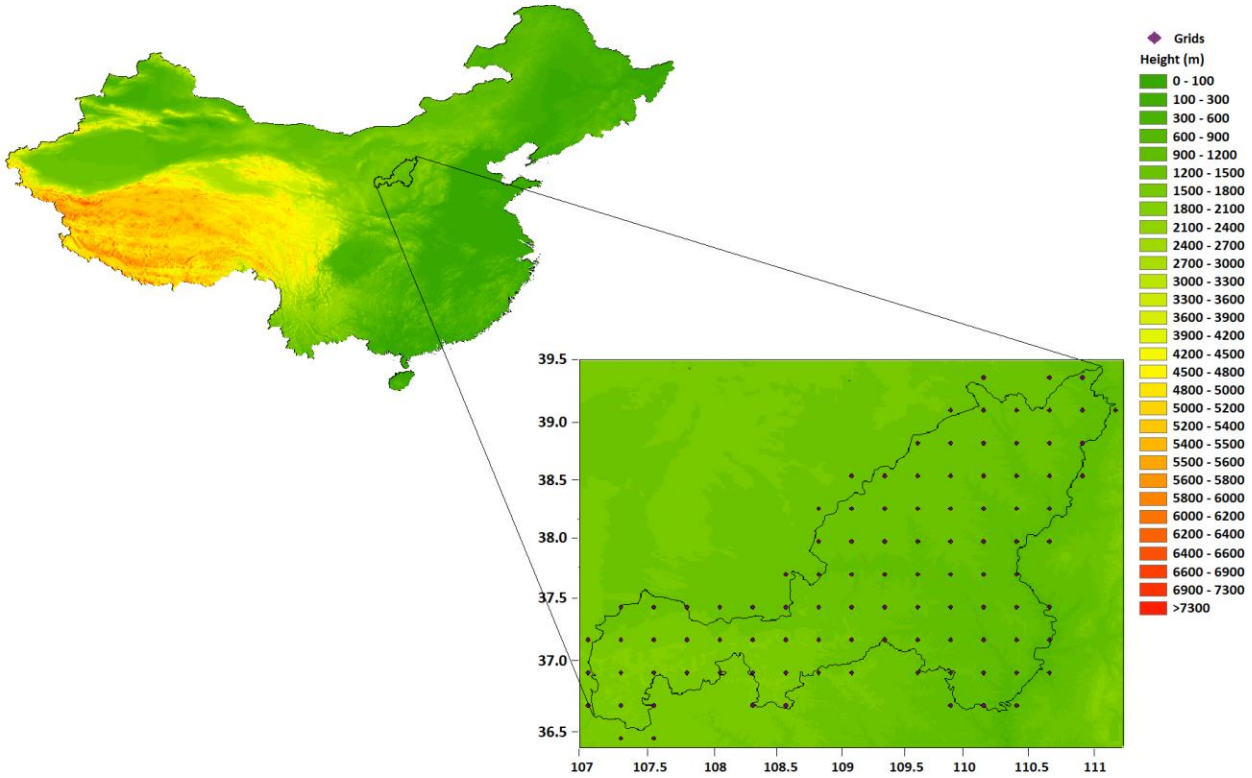

Figure 1 Map of Yulin showing the grid points considered for projection in the study.

2.2. Gauged based gridded precipitation

The GPCC full data reanalysis product of the Deutscher Wetterdienst (Becker et al., 2013; Schneider et al., 2014) was used in this study as the reference data. The GPCC precipitation amongst most other precipitation products has the advantages of (1) good data quality for hydrological studies, (2) availability for a longer period, (3) better performance as being developed using the highest number of collected precipitation records, and (4) completeness of time series for the recent decades (Ahmed, et al. 2017; Spinoni, et al. 2014). This study used the monthly precipitation data for the period 1961 – 2005. Data were collected from a total of 100 grid points to cover the whole Yulin. The location of the grid points is shown in Figure 1.

2.3 Global Climate Models

This study uses the historical and future simulations of GCMs of CMIP5 and CMIP6. The CMIPs are sets of globally coordinated GCM simulations which comprises of historical and future climate simulations assembled from different climate modeling groups. The CMIP5 offers

significant improvements compared to the CMIP3 (Taylor et al., 2012). The CMIP5 comprises of four scenarios called representative concentration pathways (RCPs). In the CMIP6, the four RCP scenarios of CMIP5, RCP2.6, RCP4.5, RCP6.0 and RCP8.5 have been updated as Shared Socioeconomic Pathways (SSPs) scenarios, SSP1-2.6, SSP2-4.5, SSP4-6.0, and SSP5-8.5 respectively. Each GCM also considers 2100 radiative forcing levels. The GCMs of CMIP6 are developed through improved emission scenarios, land use data, physical processes and model parameterization to provide more realistic projections of future climate (Eyring, et al. 2016; O'Neill, et al. 2016). In this study, historical and future simulation of 10 GCMs of CMIP5 and CMIP6 were considered. The GCMs were chosen based on their availability from the same institution. The first ensemble members for both CMIP5 and CMIP6 were considered. The GCMs chosen for this study are provided in Table 1.

Table 1. Descriptions of the GCMs of CMIP5 and CMIP6 used in this study.

Institution - Country	**CMIP5 Model Name**	**Resolution (lon/lat in °)**	**CMIP6 Model Name**	**Resolution (lon/lat in °)**
Australian Community Climate and Earth System Simulator - Australia	ACESS1.3	1.9 × 1.2	ACCESS.ESM1.5	1.9×1.2
Beijing Climate Center - China	BCC.CSM1.1(m)	1.125 × 1.125	BCC.CSM2.MR	1.1× 1.1
Canadian Centre for Climate Modelling and Analysis - Canada	CanESM2	2.8 × 2.8	CanESM5	2.8×2.8
NASA Goddard Institute for Space Studies - United States	GISS.E2.R	2.5 × 2.0	GISS.E2.1.G	2.5 × 2.0
Marchuk Institute of Numerical Mathematics - Russia	INM.CM4	2 × 1.5	INM.CM4.8	2×1.5
Institut Pierre-Simon Laplace - France	IPSL.CM5A.LR	3.75 × 1.875	IPSL.CM6A.LR	2.5× 1.3
The University of Tokyo, National Institute for Environmental Studies, and Japan Agency for Marine-Earth Science and Technology - Japan	MIROC5	1.4 × 1.4	MIROC6	1.4× 1.4
Max-Planck-Institut für Meteorologie - Germany	MPI.ESM.LR	1.9 × 1.9	MPI.ESM1.2.LR	1.9× 1.9
Meteorological Research Institute - Japan	MRI.CGCM3	1.25 × 1.25	MRI.ESM2.0	1.1× 1.1
Norwegian Meteorological Institute - Norway	NorESM1.M	2.5 × 1.875	NORESM2.MM	2.9 x 1.9

3. Methodology

The methods used in this study are described in this section. For an unbiased comparison of model performance, the GPCC and the precipitation simulations of all GCMs were re-gridded to

a uniform resolution of 1°×1° (latitude×longitude) using bilinear interpolation to have a uniform resolution. Bilinear interpolation is often conducted for transforming spatially coarse GCM data into finer data through GCM data interpolation from the four nearest neighboring grid points (Ahmed, et al. 2019; Almazroui, et al. 2020a). After selection of GCMs, the selected GCMs and the GPCC precipitation data were re-gridded to 0.25° and used for spatiotemporal projection of precipitation.

3.1 Statistical Indices

The ability of the different GCMs in reproducing the properties of GPCC precipitation at all the 100 grid points of the study area was assessed using four statistical indices: normalized root mean square error (NRMSE), Percentage of Bias (Pbias), Volumetric Efficiency (VE), and Coefficient of Determination (R^2). Besides, probability density function (pdf) and spatial relationship of the mean monthly precipitation of the different GCMs were compared with GPCC precipitation to assess their abilities in replicating the precipitation climatology of the study area. Details about the statistical metrics used in this study are as follows. The expressions used to describe statistical metrics used here: $x_{pred,i}$ and $x_{obs,i}$ are the i-th GCM and GPCC data. The magnitude of the errors in estimation can be summarized by NRMSE (Willmott 1982). It is a normalized statistic that provides a relative magnitude of the residual variance to the variance of the measured data. Smaller NRMSE values (preferably zero) indicate better performance of the model. NRMSE is defined as follows

$$NRMSE = \frac{\left[\frac{1}{n}\sum_{i=1}^{n}\left(x_{pred,i}-x_{obs,i}\right)^2\right]^{1/2}}{\frac{1}{n}\sum_{i=1}^{n}\left(x_{pred,i}\right)} \quad (1)$$

The tendency of GCM to underestimate or overestimate the GPCC precipitation is measured using Pbias. Model performance is better when the Pbias is closer to zero. The PBIAS is a statistical metric that gives the estimate of over estimation or under prediction of a model (Wagena, et al. 2018). The evaluation of Pbias is conducted as follows.

$$Pbias = 100 \times \left[\frac{\sum_{i=1}^{n}\left(x_{pred,i}-x_{obs,i}\right)}{\sum_{i=1}^{n} x_{pred,i}}\right] \quad (2)$$

The VE measures the ratio between GCM and GPCC precipitation volumes over a period, where a VE value of 1 indicates a perfect estimation. It can be calculated using the following equation.

$$VE = 1 - \frac{\sum_{i=1}^{n}(x_{pred,i} - x_{obs,i})}{\sum_{i=1}^{n} x_{obs,i}} \quad (3)$$

The R^2 can be defined as the square of the Pearson's product-moment correlation coefficient (i.e. $R^2 = r^2$) describing the proportion of the total variance in the GPCC precipitation which is explainable by GCM (Legates and McCabe Jr 1999). R^2 values can range between -1.0 and 1.0, in which the higher absolute value indicates a better agreement. Computation of R^2 is as follows.

$$R^2 = \frac{\sum_{i=1}^{N}\left(x_{obs,i} - \overline{x_{obs}}\right)\left(x_{\mathrm{Pred},i} - \overline{x_{\mathrm{Pred}}}\right)}{\sqrt{\sum_{i=1}^{N}\left(x_{\mathrm{Pred},i} - \overline{x_{\mathrm{Pred}}}\right)^2 \sum_{i=1}^{N}\left(x_{obs,i} - \overline{x_{obs}}\right)^2}} \quad (4)$$

3.2 Downscaling of precipitation of selected GCMs of CMIP5 and CMIP6

The linear scaling (LS) method was applied for the downscaling of the selected GCMs. LS (Lenderink, et al. (2007) uses the monthly correction values obtained from the difference in GPCC and GCMs simulated monthly precipitation for the reference period. The monthly scaling factor is then applied to raw GCM data. The monthly precipitation, P is corrected using the following equation:

$$P^* = \alpha P \quad (5)$$

where $\alpha = P_o/P_s$ (6)

P_o is the monthly mean of GPCC precipitation whereas P_s is the monthly mean of the GCM simulated precipitation. LS method requires less information such as only monthly data to calculate the scaling factor (Lafon, et al. 2013) and thus, widely used for precipitation downscaling.

4. Results

4.1 Performance assessment of GCMs using statistical metrics

The results of the statistics used for the performance evaluation of different historical GCMs are presented in Table 2. It shows a variation in the performances of different GCMs. For CMIP5,

194 the GCMs with the best performance metrics are ACESS1.3, BCC.CSM1.1(m), IPSL.CM5A.LR,
195 and MIROC5. The GCMs of the same institutions also showed good performances for CMIP6
196 except for ACCESS.ESM1.5 which showed a relatively poor performance.
197
198 Table 2. Statistical metrics showing the performances of GCMs of CMIP5 and CMIP6 in replicating GPCC
199 precipitation over Yulin (Best metrics are presented in bold).

CMIP5					CMIP6				
GCM	**NRMSE**	**Pbias**	**VE**	**R^2**	**GCM**	**NRMSE**	**Pbias**	**VE**	**R^2**
ACESS1.3	**76.3**	**10.9**	0.68	**0.73**	ACCESS.ESM1.5	154.4	23.8	0.67	**0.77**
BCC.CSM1.1(m)	**144.8**	**21.2**	**0.79**	**0.79**	BCC.CSM2.MR	**115**	**19.8**	**0.8**	**0.63**
CanESM2	292.9	49.8	0.5	0.16	CanESM5	136.1	23.7	0.73	0.46
GISS.E2.R	**135.8**	29.1	0.68	0.22	GISS.E2.1.G	175.8	53.3	0.47	0.04
INM.CM4	274.7	38.8	0.61	0.46	INM.CM4.8	279.9	41.5	0.59	0.45
IPSL.CM5A.LR	**81.0**	**-4.5**	**0.77**	0.36	IPSL.CM6A.LR	**70.2**	**6.1**	**0.8**	0.59
MIROC5	177.2	**27.5**	**0.72**	**0.76**	MIROC6	181.6	**23.3**	0.72	**0.65**
MPI.ESM.LR	174.3	35.5	0.65	0.41	MPI.ESM1.2.LR	**123.3**	23.6	**0.76**	0.54
MRI.CGCM3	173.8	-44.6	**0.70**	**0.85**	MRI.ESM2.0	**85.8**	**-21.3**	**0.78**	**0.78**
NorESM1.M	397.3	55.1	0.45	0.21	NORESM2.MM	182.6	29.8	0.7	0.62

200
201 *4.2 Spatial relationship between GCMs and GPCC precipitations*
202 The ability of different GCMs in replicating the spatial distribution of GPCC precipitation for the
203 study area are presented in Figure 2. The performances of the GCMs were found to vary widely
204 in reproducing the GPCC precipitation. Among CMIP5 GCMs, the highest overestimations were
205 by CanESM2 and NorESM1-M, while an underestimation was by MRI-CGCM3 followed by
206 IPSL-CM5A-LR in some parts. For CMIP6, GISS-E2-1G showed the highest overestimation of
207 precipitation. Generally, the GCMs with better performance metrics (Table 2) showed better
208 skills in replicating the precipitation climatology of GPCC for the study area.

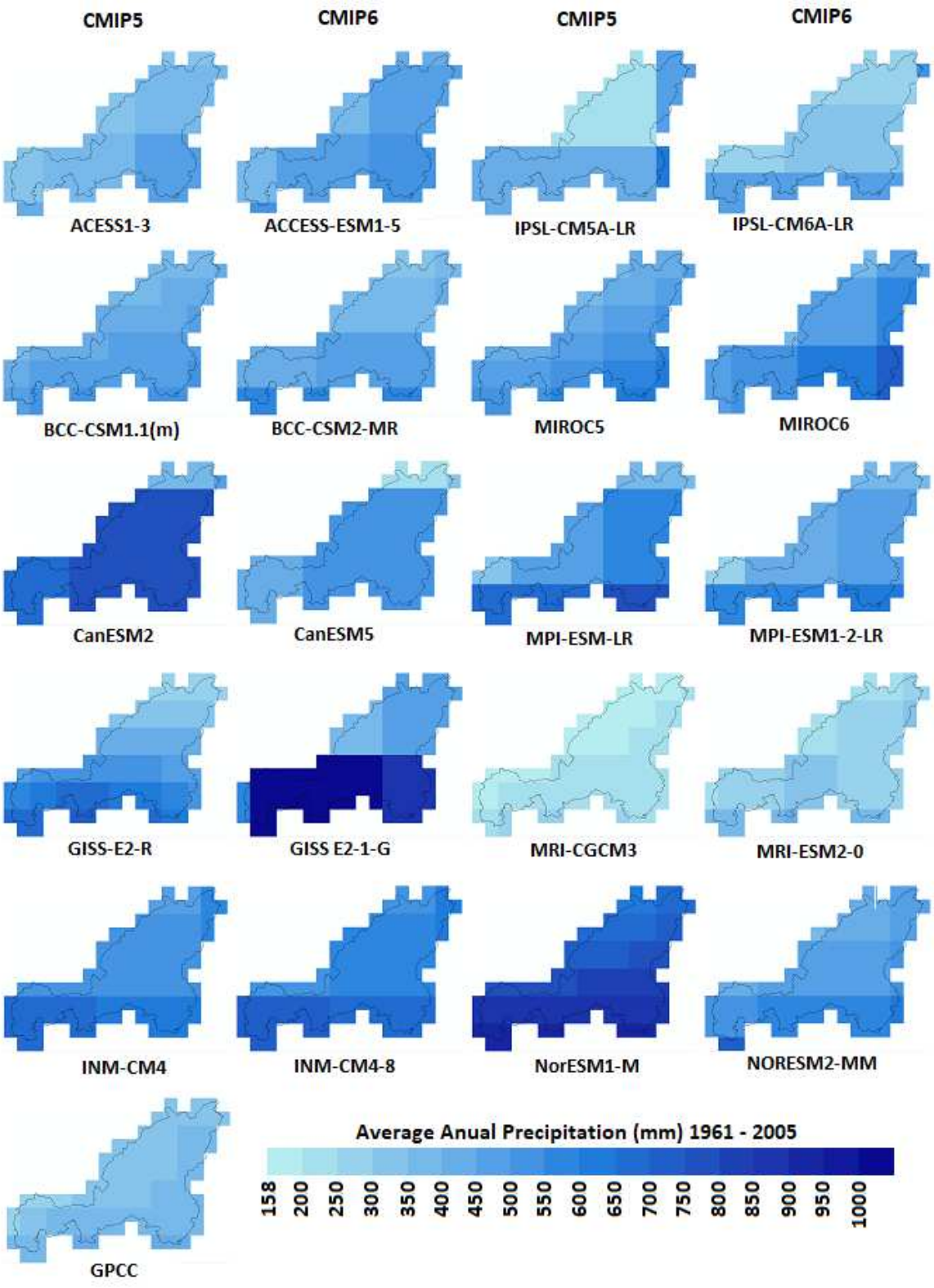

Figure 2 Spatial distribution of average annual precipitation of GCMs of CMIP5 and CMIP6 compared to that of GPCC during 1961–2005.

4.3 Comparison using probability density function

The PDFs of monthly GCM precipitation was compared with the PDF of GPCC precipitation for the study area. The results for CMIP5 and CMIP6 are presented in Figure 3(a) and 3(b) respectively. Figures show that most GCMs were able to replicate the precipitation properties of the GPCC, especially the skewness. However, the distribution of precipitation was found better for the GCMs which showed a better performance in terms of statistical metrics presented in Table 2.

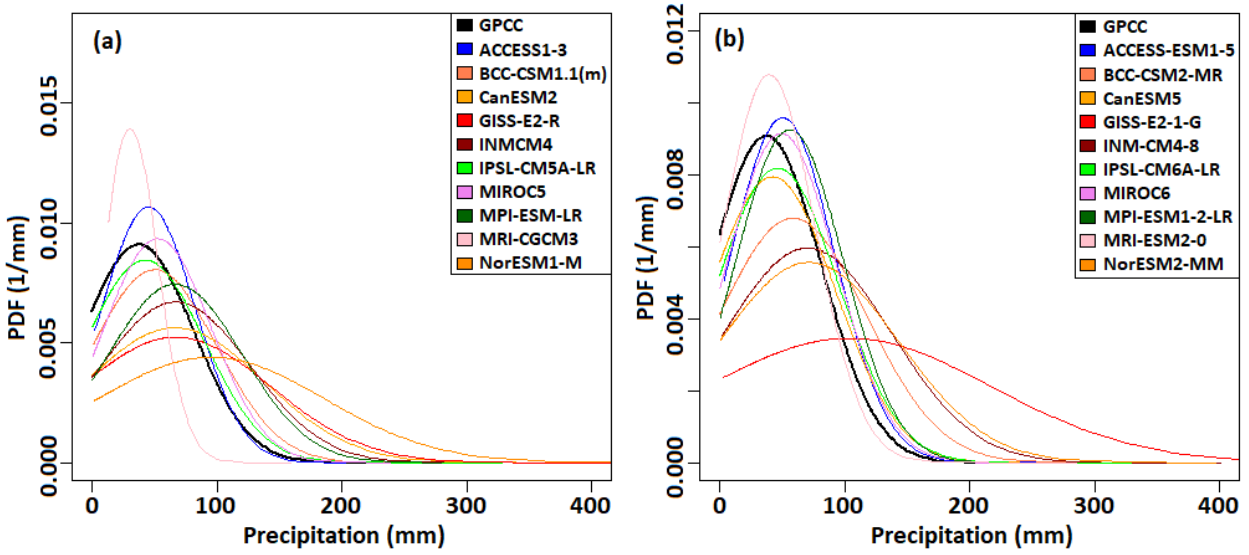

Figure 3 Probability density function of monthly precipitations of GPCC and the GCMs of (a) CMIP5 and (b) CMIP6.

4.4 Comparison of GCMs in reproducing monthly mean precipitation

The mean monthly GCM precipitation was compared with mean monthly GPCC precipitation for the period 1961–2005. Obtained results for the GCMs of CMIP5 and CMIP6 are presented in Figure 4(a) and (b) respectively. There was a variation in the estimation of GPCC precipitation by the GCMs, especially during the wet season. CanESM2 and NorESM1-M of CMIP5 overestimated the precipitation for all the months, while an underestimation was by MRI-CGCM3. For the CMIP6, overestimation was by GISS-E2-1-2G and underestimation by MRI-ESM2-0 and IPSL-CM5A-LR, especially during the wet period. Though most of the

CMIP6 GCMs were found to overestimate the GPCC precipitation, overall they were found more capable in replicating the mean monthly precipitation of GPCC compared to CMIP5 GCMs.

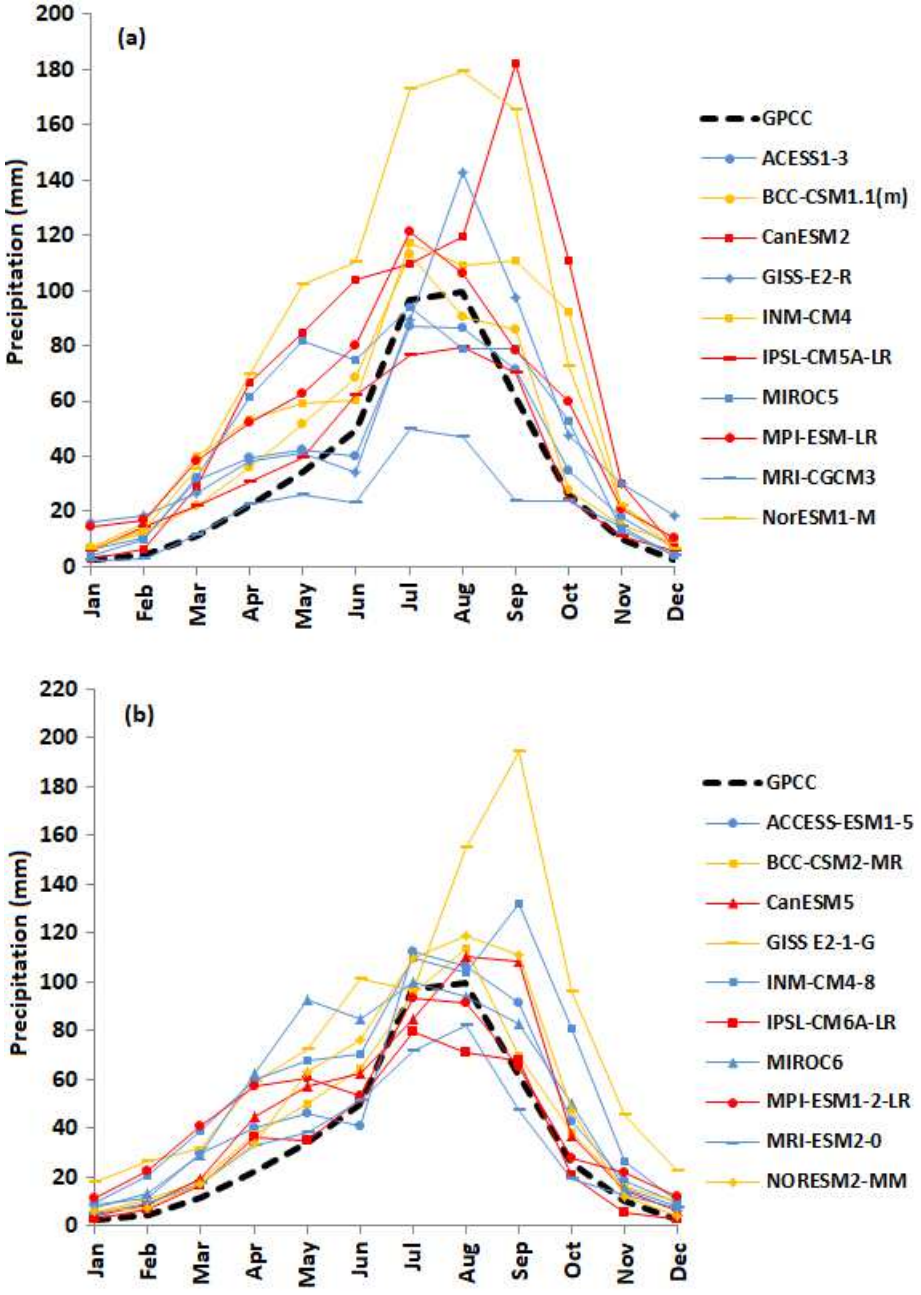

Figure 4 Comparison of mean monthly precipitation of GCMs of (a) CMIP5 and (b) CMIP6 with that of GPCC precipitation.

4.5 Selection of the best performing GCMs

The performance of the GCMs based on statistical indices and replication of PDF, and spatial precipitation distribution patterns were considered. Based on the statistics, BCC.CSM1.1(m), IPSL.CM5A.LR, and MIROC5 were the better performing GCMs for both CMIP5 and CMIP6. Besides, ACESS1.3 showed overall a better performance compared to the rest of the CMIP5 GCMs, while its equivalent under CMIP6 showed a poor performance than MRI.ESM2.0. As CMIP6 is a more recent simulation, the MRI.CGCM3 for CMIP5 and its equivalent GCM for MICP6, MRI.ESM2.0 were prioritized as the fourth model for projection of precipitation.

4.7 Projection of precipitation from the selected GCMs of CMIP5 and CMIP6

The spatial projections of precipitation for the study area by CMIP5 GCMs for RCP 4.5 and CMIP6 GCMs for SSP2-4.5 for two future periods, 2021–2060 and 2061 – 2100 are presented in Figure 5. Large heterogeneity in precipitation changes was projected by different GCMs for RCPs and SSPs and the two projection periods. During 2021 – 2060, the highest decrease in precipitation was projected by MRI-ESM-2-0 for SSP2-4.5 while the highest decrease for RCP 4.5 was projected by MIROC5. For the same period, BCC-CSM2-MR projected an increase in precipitation by 1.2% at the extreme west of the study area. Percentage change in precipitation was in the range of -14.0 – 0.0% for RCP4.5 while it was -22.0 – 1.2% for SSP2-4.5. During 2061 – 2100, all the GCMs projected decreases in precipitation, with the highest decrease of -29.7 − -22.0% by MRI-ESM-2-0 for SSP2-4.5 and -28.0 − -20.0% by MIROC5 for RCP4.5. The lowest decrease during this period was projected by MRI-CGCM3 and BCC-CSM2-MR for RCP4.5 and SSP2-4.5 respectively.

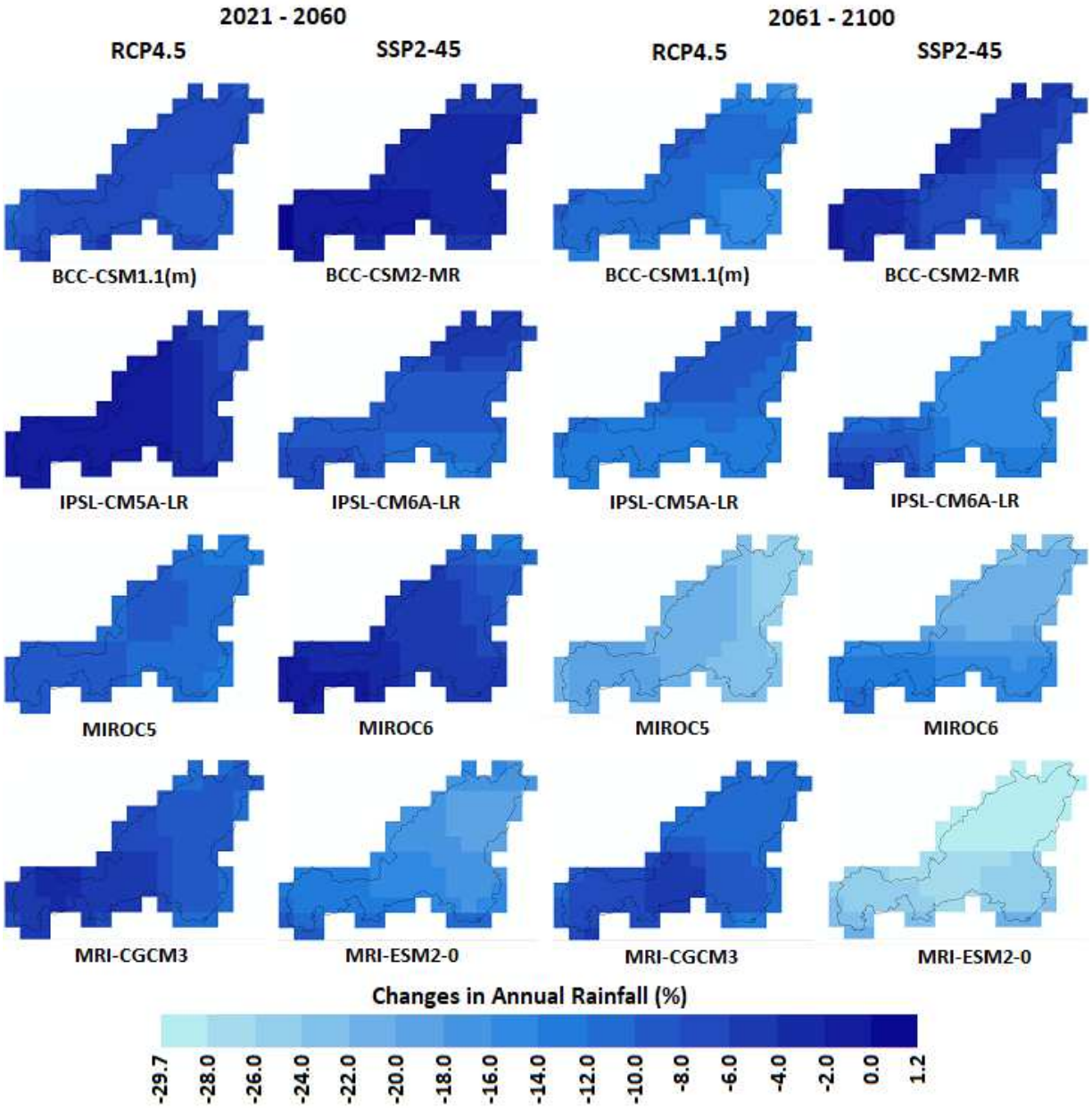

Figure 5. Spatial distribution of projected precipitation by the GCMs of CMIP5 and CMIP6 during 2021–2060 and 2061–2100 for RCP4.5 and SSP2-4.5.

The spatial distribution of projected precipitation in the study area by CMIP5 GCMs for RCP 8.5 and CMIP6 GCMs for SSP5-8.5 for the periods 2021–2060 and 2061–2100 are presented in Figure 6. Compared to RCP 4.5 and SSP2-4.5, RCP8.5 and SSP5-8.5 showed higher decreases in precipitation. During 2021 – 2060, the projected decrease in precipitation was in the range of -17.0 − -2.0% by the CMIP5 GCMs for RCP8.5 while the decrease was projected

between -32.0 and 0.0% by the CMIP6 GCMs for SSP5-8.5. Increases in precipitation of 0.0 − 12.3% were noticed only for IPSL-CM5A-LR for RCP8.5. During 2061 – 2100, the decrease in precipitation was projected the highest by MIROC5 (-40.2 − -29.0%) for RCP8.5 and IPSL-CM6A-LR (-40.2 − -26.0%) for SSP5-8.5.

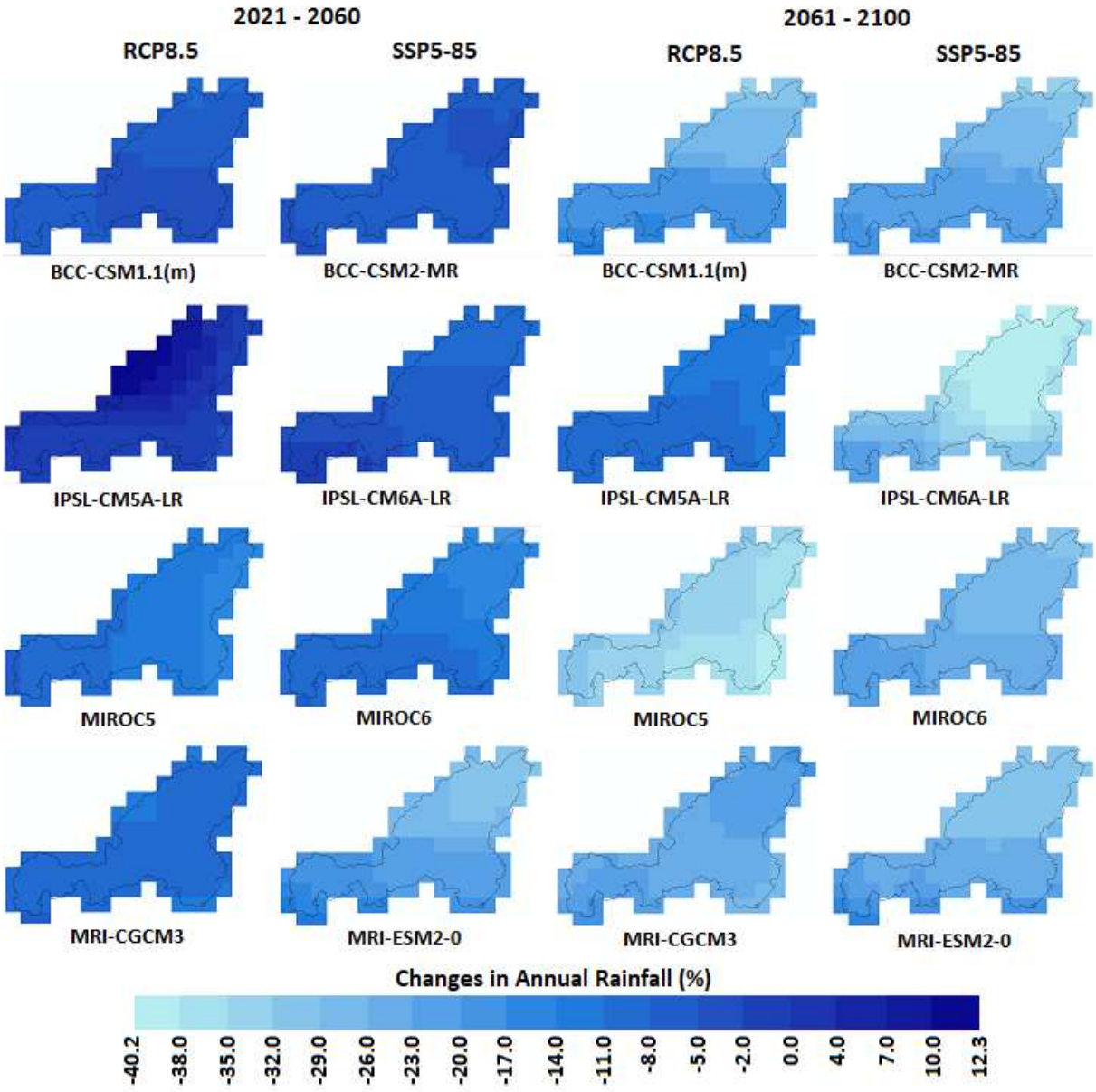

Figure 6. Spatial distribution of projected precipitation by the GCMs of CMIP5 and CMIP6 during 2021–2060 and 2061–2100 for RCP8.5 and SSP5-8.5.

5. Discussion

Climate change remains a major challenge in many parts of the globe as they have devastating impacts on several sectors. Many studies have shown that the expected changes in climate will result in increased temperatures and more erratic precipitations in many parts of the world. Projection of precipitation under CMIP5 in Nigeria showed that while precipitation will increase in some parts of the country, particularly the semi-arid and arid regions where they are usually low, the other parts where they used to be higher will experience decreases (Shiru, et al. 2019b). (Homsi, et al. 2020) used CMIP5 GCMs in Syria and showed that precipitation would increase by up to 87% in some parts and decrease by up to -85% in the coastal areas. Many other studies have also shown both increase and decrease in precipitation in many parts of the world using CMIP5 GCMs (Iqbal, et al. 2020; Narsey, et al. 2020; Shiru and Park 2020; Ullah, et al. 2020).

The studies for the recently released CMIP6 GCMs have also shown such changes in precipitation. The study conducted over South Asian countries Almazroui, et al. (2020c) showed that the annual mean precipitation will increase by 27.3% in India, 18.9% in Bhutan, 26.4% in Pakistan, 19.5% in Nepal, 25.1% in Sri Lanka and 17.1% in Bangladesh in the last part of the century under SSP5-8.5 scenario. Over Africa, (Almazroui, et al. 2020b) projected precipitation under CMIP6 and showed that while the northern and the southern parts of Africa are analyzed to witness a reduction in precipitation, the central parts are expected to have increases of 6.2%, 6.8%, and 9.5% for SSP1-2.6, SSP2-4.5, and SSP5-8.5, respectively.

In China, studies showed variations in the projected precipitations for both CMIP5 and CMIP6 with some studies showing mostly increases while others showed a simultaneous increase and decrease depending on the region. The annual precipitation was projected to increase significantly relative to the present day for CMIP5 (Chen 2013). This study revealed that the increase of precipitation in the Northwest of China is primarily due to the increase in light showers while the increases in precipitation in the north and northeastern parts are due to an increase in medium precipitation. The increases in precipitation are expected in the southern parts of China due to an increment in heavy precipitation. Zhou, et al. (2019) showed both increases and decreases in daily precipitation under different warming conditions over China using CMIP5. The increase in warming of 1.5°C was projected to cause an increase in the

frequency and intensity of precipitation in northeast China, north China, and the Qinghai–Tibet Plateau while there would be a decrease in total precipitation in south China and southwest China. The number of wet days were projected to increase in the north while the decreases in the south under 2°C.

The projection of the changes in precipitation over northwestern China for CMIP6 (Su-Yuan, et al. 2020) showed that there would be lesser warming compared to that previously expected, which would affect the patterns in precipitation changes. Unlike in the historical period (1850 – 2014) when the rate of warming was 0.05°C per decade, the annual mean temperature is projected to increase up to 0.06°C, 0.26°C and 0.59°C per decade for SSP1-2.6, SSP2-4.5 and SSP5-8.5, respectively for the period 2015–2099. The total annual precipitation for the area is projected to increase by 5.6, 6.4 and 8.0 mm/decade for SSP1-2.6, SSP2-4.5 and SSP5-8.5, respectively.

In this study, both increases and decreases in precipitation are projected for the study area. Zhou, et al. (2019) projected the increases in precipitation over China, except some northwestern parts where Yulin belongs, which supports the findings of this study. The projected the increases in some parts of the study area are also corroborated by other studies.

6. Conclusions

This study compares the projections of precipitation by CMIP5 and CMIP6 GCMs over Yulin city of China. Different statistical and graphical metrics were used in assessing the ability of 10 GCMs in replicating the precipitation properties of the study area. Finally, four GCMs having the highest ability in replicating the properties of GPCC precipitation were selected for the projection of precipitation over the study area. This study revealed that ACESS1.3, BCC.CSM1.1(m), IPSL.CM5A.LR and MIROC5 of CMIP5 and their equivalents in CMIP6, BCC-CSM2-MR, IPSL-CM6A-LR, MRI.ESM2.0 and MIROC6 have better abilities in replicating historical precipitation properties over Yulin. Projection of precipitation showed an overall decrease in precipitation over Yulin by the GCMs of both CMIPs. The decrease in precipitation would be more in the far future compared to the near future. The expected decreases in precipitation can increase the frequency and intensity of droughts in the area. The

findings of the study can be used as a guide in the development of adaptation and mitigation measures against climate change in the area. In the future, more GCMs common to both CMIP5 and CMIP6 can be employed when they will be available for CMIP6 for the selection of best performing GCMs. Besides, a more reliable approach can be utilized for the selection of GCMs to avoid the dispute in selection using conventional statistical metrics.

Funding Statement

This work was supported under the framework of international cooperation program managed by the National Research Foundation of Korea (2019K2A9A2A06018602).

References

Ahmed, K., Shahid, S., Ali, R.O., Harun, S., Wang, X., 2017. Evaluation of the performance of gridded precipitation products over Balochistan Province, Pakistan. Desalination 1, 14.

Ahmed, K., Shahid, S., Sachindra, D., Nawaz, N., Chung, E.-S., 2019. Fidelity assessment of general circulation model simulated precipitation and temperature over Pakistan using a feature selection method. Journal of hydrology 573, 281-298.

Alamgir, M., Mohsenipour, M., Homsi, R., Wang, X., Shahid, S., Shiru, M.S., Alias, N.E., Yuzir, A., 2019. Parametric Assessment of Seasonal Drought Risk to Crop Production in Bangladesh. Sustainability 11, 1442.

Almazroui, M., Islam, M.N., Saeed, S., Saeed, F., Ismail, M., 2020a. Future Changes in Climate over the Arabian Peninsula based on CMIP6 Multimodel Simulations. Earth Systems and Environment, 1-20.

Almazroui, M., Saeed, F., Saeed, S., Islam, M.N., Ismail, M., Klutse, N.A.B., Siddiqui, M.H., 2020b. Projected change in temperature and precipitation over Africa from CMIP6. Earth Systems and Environment, 1-21.

Almazroui, M., Saeed, S., Saeed, F., Islam, M.N., Ismail, M., 2020c. Projections of precipitation and temperature over the South Asian countries in CMIP6. Earth Systems and Environment 4, 297-320.

Ayugi, B., Tan, G., Rouyun, N., Zeyao, D., Ojara, M., Mumo, L., Babaousmail, H., Ongoma, V., 2020. Evaluation of Meteorological Drought and Flood Scenarios over Kenya, East Africa. Atmosphere 11, 307.

Chen, H., 2013. Projected change in extreme rainfall events in China by the end of the 21st century using CMIP5 models. Chinese Science Bulletin 58, 1462-1472.

Chen, J., Brissette, F.P., Lucas-Picher, P., Caya, D., 2017. Impacts of weighting climate models for hydro-meteorological climate change studies. Journal of Hydrology 549, 534-546.

China-Daily, 2012. Flooding in Shaanxi province kills 11. http://europe.chinadaily.com.cn/china/2012-07/30/content_15632933.htm Updated: 2012-07-30 22:41 Accessed:12/10/2020.

Eyring, V., Bony, S., Meehl, G.A., Senior, C.A., Stevens, B., Stouffer, R.J., Taylor, K.E., 2016. Overview of the Coupled Model Intercomparison Project Phase 6 (CMIP6) experimental design and organization. Geoscientific Model Development 9, 1937-1958.

Fowler, H.J., Blenkinsop, S., Tebaldi, C., 2007. Linking climate change modelling to impacts studies: recent advances in downscaling techniques for hydrological modelling. International Journal of Climatology: A Journal of the Royal Meteorological Society 27, 1547-1578.
He, Y., He, S., Hu, Z., Qin, Y., Zhang, Y., 2018. The devastating 26 July 2017 floods in Yulin City, Northern Shaanxi, China. Geomatics, Natural Hazards and Risk 9, 70-78.
Homsi, R., Shiru, M.S., Shahid, S., Ismail, T., Harun, S.B., Al-Ansari, N., Chau, K.-W., Yaseen, Z.M., 2020. Precipitation projection using a CMIP5 GCM ensemble model: a regional investigation of Syria. Engineering Applications of Computational Fluid Mechanics 14, 90-106.
Huang, C., Shen, J.J., Zhou, M., Lee, G.C., 2015. Force-based and displacement-based reliability assessment approaches for highway bridges under multiple hazard actions. Journal of Traffic and Transportation Engineering (English Edition) 2, 223-232.
Iqbal, Z., Shahid, S., Ahmed, K., Ismail, T., Khan, N., Virk, Z.T., Johar, W., 2020. Evaluation of global climate models for precipitation projection in sub-Himalaya region of Pakistan. Atmospheric Research, 105061.
Kang, S., Eltahir, E.A., 2018. North China Plain threatened by deadly heatwaves due to climate change and irrigation. Nature communications 9, 1-9.
Khan, N., Shahid, S., Ismail, T., Ahmed, K., Nawaz, N., 2019. Trends in heat wave related indices in Pakistan. Stochastic environmental research and risk assessment 33, 287-302.
Kim, G.-U., Seo, K.-H., Chen, D., 2019. Climate change over the Mediterranean and current destruction of marine ecosystem. Scientific reports 9.
Lafon, T., Dadson, S., Buys, G., Prudhomme, C., 2013. Bias correction of daily precipitation simulated by a regional climate model: a comparison of methods. International Journal of Climatology 33, 1367-1381.
Legates, D.R., McCabe Jr, G.J., 1999. Evaluating the use of "goodness-of-fit" measures in hydrologic and hydroclimatic model validation. Water resources research 35, 233-241.
Lenderink, G., Buishand, A., Deursen, W.v., 2007. Estimates of future discharges of the river Rhine using two scenario methodologies: direct versus delta approach. Hydrology and Earth System Sciences 11, 1145-1159.
Manawi, S.M.A., Nasir, K.A.M., Shiru, M.S., Hotaki, S.F., Sediqi, M.N., 2020. Urban Flooding in the Northern Part of Kabul City: Causes and Mitigation. Earth Systems and Environment, 1-12.
Narsey, S., Brown, J., Colman, R., Delage, F., Power, S., Moise, A., Zhang, H., 2020. Climate change projections for the Australian monsoon from CMIP6 models. Geophysical Research Letters 47, e2019GL086816.
O'Neill, B.C., Tebaldi, C., Van Vuuren, D.P., Eyring, V., Friedlingstein, P., Hurtt, G., Knutti, R., Kriegler, E., Lamarque, J.-F., Lowe, J., 2016. The scenario model intercomparison project (ScenarioMIP) for CMIP6.
Onyutha, C., Tabari, H., Rutkowska, A., Nyeko-Ogiramoi, P., Willems, P., 2016. Comparison of different statistical downscaling methods for climate change rainfall projections over the Lake Victoria basin considering CMIP3 and CMIP5. Journal of hydro-environment research 12, 31-45.
Pérez-Ruiz, C.L., Badano, E.I., Rodas-Ortiz, J.P., Delgado-Sánchez, P., Flores, J., Douterlungne, D., Flores-Cano, J.A., 2018. Climate change in forest ecosystems: a field experiment addressing the effects of raising temperature and reduced rainfall on early life cycle stages of oaks. Acta oecologica 92, 35-43.
Pour, S.H., Shahid, S., Chung, E.-S., Wang, X.-J., 2018. Model output statistics downscaling using support vector machine for the projection of spatial and temporal changes in rainfall of Bangladesh. Atmospheric research 213, 149-162.
Rahman, M., Ningsheng, C., Islam, M.M., Dewan, A., Iqbal, J., Washakh, R.M.A., Shufeng, T., 2019. Flood Susceptibility Assessment in Bangladesh Using Machine Learning and Multi-criteria Decision Analysis. Earth Systems and Environment 3, 585-601.

Rivera, J.A., Arnould, G., 2020. Evaluation of the ability of CMIP6 models to simulate precipitation over Southwestern South America: Climatic features and long-term trends (1901–2014). Atmospheric Research, 104953.
Sa'adi, Z., Shiru, M.S., Shahid, S., Ismail, T., 2019. Selection of general circulation models for the projections of spatio-temporal changes in temperature of Borneo Island based on CMIP5. Theoretical and Applied Climatology, 1-21.
Salman, S.A., Shahid, S., Ismail, T., Ahmed, K., Wang, X.-J., 2018. Selection of climate models for projection of spatiotemporal changes in temperature of Iraq with uncertainties. Atmospheric research 213, 509-522.
Satyanarayana, G., Rao, D.B., 2020. Phenology of heat waves over India. Atmospheric Research, 105078.
Shiru, M.S., Chung, E.-S., Shahid, S., Alias, N., 2020. GCM selection and temperature projection of Nigeria under different RCPs of the CMIP5 GCMS. Theoretical and Applied Climatology 141, 1611-1627.
Shiru, M.S., Park, I., 2020. Comparison of Ensembles Projections of Rainfall from Four Bias Correction Methods over Nigeria. Water 12, 3044.
Shiru, M.S., Shahid, S., Chung, E.-S., Alias, N., 2019a. Changing characteristics of meteorological droughts in Nigeria during 1901–2010. Atmospheric Research 223, 60-73.
Shiru, M.S., Shahid, S., Chung, E.-S., Alias, N., Scherer, L., 2019b. A MCDM-based framework for selection of general circulation models and projection of spatio-temporal rainfall changes: A case study of Nigeria. Atmospheric Research 225, 1-16.
Spinoni, J., Naumann, G., Carrao, H., Barbosa, P., Vogt, J., 2014. World drought frequency, duration, and severity for 1951–2010. International Journal of Climatology 34, 2792-2804.
Sreelatha, K., Anand Raj, P., 2019. Ranking of CMIP5-based global climate models using standard performance metrics for Telangana region in the southern part of India. ISH Journal of Hydraulic Engineering, 1-10.
Su-Yuan, L., Li-Juan, M., Zhi-Hong, J., Guo-Jie, W., Raj, G.K., Jing, Z., Hui, Z., Ke, F., Yu, H., Chun, L., 2020. Projected drought conditions in Northwest China with CMIP6 models under combined SSPs and RCPs for 2015–2099. Advances in Climate Change Research.
Taylor, K.E., Stouffer, R.J., Meehl, G.A., 2012. An overview of CMIP5 and the experiment design. Bulletin of the American Meteorological Society 93, 485-498.
Ullah, S., You, Q., Zhang, Y., Bhatti, A.S., Ullah, W., Hagan, D.F.T., Ali, A., Ali, G., Jan, M.A., Khan, S.N., 2020. Evaluation of CMIP5 models and projected changes in temperatures over South Asia under global warming of 1.5 oC, 2 oC, and 3 oC. Atmospheric Research 246, 105122.
Wagena, M.B., Collick, A.S., Ross, A.C., Najjar, R.G., Rau, B., Sommerlot, A.R., Fuka, D.R., Kleinman, P.J., Easton, Z.M., 2018. Impact of climate change and climate anomalies on hydrologic and biogeochemical processes in an agricultural catchment of the Chesapeake Bay watershed, USA. Science of the Total Environment 637, 1443-1454.
Wang, T., 2016. Vegetation NDVI change and its relationship with climate change and human activities in Yulin, Shaanxi Province of China. Journal of Geoscience and Environment Protection 4, 28.
Wang, Y., Kong, Y., Chen, H., Ding, Y., 2020. Spatial-temporal characteristics of drought detected from meteorological data with high resolution in Shaanxi Province, China. Journal of Arid Land 12, 561-579.
Willmott, C.J., 1982. Some comments on the evaluation of model performance. Bulletin of the American Meteorological Society 63, 1309-1313.
Yang, Y., Du, J., Cheng, L., Xu, W., 2017. Applicability of TRMM satellite precipitation in driving hydrological model for identifying flood events: a case study in the Xiangjiang River Basin, China. Natural Hazards 87, 1489-1505.
Yin, Y., Zhang, L., Wang, X., Xu, W., Yu, W., Zhu, Y., 2020. Meteorological Drought Changes and Related Circulation Characteristics in Yulin City of the Northern Shaanxi from 1961 to 2015. Atmosphere 11, 1196.

Zha, Y., Liu, Y., Deng, X., 2008. A landscape approach to quantifying land cover changes in Yulin, Northwest China. Environmental Monitoring and Assessment 138, 139-147.
Zhou, M., Zhou, G., Lv, X., Zhou, L., Ji, Y., 2019. Global warming from 1.5 to 2° C will lead to increase in precipitation intensity in China. International Journal of Climatology 39, 2351-2361.

Author Contributions

Conceptualization, Mohammed Sanusi Shiru, Eun-Sung Chung; Formal analysis, Mohammed Sanusi Shiru, Eun-Sung Chung, Shamsuddin Shahid, and Xiao-Jun Wang; Methodology, Mohammed Sanusi Shiru, Eun-Sung Chung, Shamsuddin Shahid, and Xiao-Jun Wang, Writing – original draft, Mohammed Sanusi Shiru, Eun-Sung Chung; Writing – review & editing, Mohammed Sanusi Shiru, Eun-Sung Chung, Shamsuddin Shahid, and Xiao-Jun Wang.

Ethical approval

This article does not contain any studies with human or animal participants performed by any of the authors.

Consent to Particupate

The authors declare that they have consent to participate in this paper.

Consent to Publish

The authors declare that they have consent to publish in this journal.

Conflicts of interests

The authors declare that they have no known competing interests that authors must disclose all affiliations, funding sources, financial or personal relationships that could be perceived as potential sources of bias.

Availability of data and materials

The authors can support all relevant data if requested.